

## IV RUSSIAN CONFERENCE WITH THE PARTICIPATION OF CIS COUNTRIES ON THE SCIENTIFIC BASES OF CATALYST PREPARATION AND TECHNOLOGY

# Reasons for the Deactivation of Vanadia–Titania Catalysts for Partial Durene Oxidation during Prolonged Performance

B. I. Kutepov\* and B. S. Bal'zhinimaev\*\*

\* Institute of Petrochemistry and Catalysis, Academy of Sciences of Bashkortostan and Ufa Scientific Center,  
Russian Academy of Sciences, Ufa, Bashkortostan, Russia

\*\* Boreskov Institute of Catalysis, Siberian Division, Russian Academy of Sciences, Novosibirsk, 630090 Russia

Received September 18, 2000

**Abstract**—The catalytic properties of vanadia–titania catalysts and the reasons for their change in the course of durene oxidation to pyromellitic dianhydride are studied. The catalysts differ in preparation conditions and the composition of the active component film deposited on a nonporous support. The stability of the catalytic properties in the reaction medium of durene oxidation is mainly determined by the properties of titania precursors.

## INTRODUCTION

Pyromellitic dianhydride (PMDA) is a raw material for the manufacturing of polyimides with unique properties. PMDA can be prepared by heterogeneous catalytic gas-phase durene oxidation [1]. The simplest catalysts for this process are fused  $V_2O_5$  and  $V_2O_5$  supported on a nonporous carrier (corundum and silicon carbide). To enhance the activity and selectivity of the catalyst, the additives W, P, Sn, Ti, Ag, Mo, Cu, Na, K, Rb, and Cr have been proposed [2].

Durene oxidation to PMDA resembles *o*-xylene oxidation to phthalic anhydride over vanadia–titania systems deposited as a thin film on the surface of nonporous supports. These catalysts are the most selective and therefore recommended for PMDA synthesis [3–5].

It has been found that the structure of the active phase in the V–Ti systems depends essentially on the  $V_2O_5$  concentration ( $C_V$ ) and preparation conditions [6–17]. The presence of isolated (tetrahedrally or octahedrally coordinated) vanadium cations, cluster oxide species of various sizes, and a disperse  $V_2O_5$  phase has been assumed. Note that the structures of model systems containing one or several layers of an active component have been described in these works, whereas the catalysts recommended for industrial use contain 5.0 to 25.0 wt %  $V_2O_5$ . In addition, data reported previously only deal with the initial state of an active component in the catalyst, and this state may change under the action of the reaction medium [18].

Our aim was to study the effect of prolonged exposure to the reaction medium in durene oxidation to PMDA on the catalytic properties, structure, phase composition, and valent state of vanadia–titania systems which differ in their composition and preparation conditions.

## EXPERIMENTAL

To prepare catalysts, we used  $V_2O_5$ , aqueous solutions of  $NH_4VO_3$  and  $VOC_2O_4$ , Ti(IV) oxide of (A1 trademark, anatase), which is used for commercial KS and KT catalysts, and hydrated titania  $TiO_2 \cdot nH_2O$ . Samples of film catalysts were prepared as follows. Porcelain balls with a diameter of 8 mm were placed into a heated cylinder, and suspended  $TiO_2$  (anatase) in a  $VOC_2O_4$  or  $NH_4VO_3$  solution heated to 90°C was introduced by a pneumatic injector. Various concentrations of active components in the catalysts were achieved by changing the composition of the suspension. The second procedure differed only in the composition of the aqueous suspension containing  $V_2O_5$ ,  $TiO_2$  (anatase), and  $TiO_2 \cdot nH_2O$  in different ratios. Only one sample prepared by sputtering the suspension of the above components with the 1 : 3 : 1 weight ratio (22 wt %  $V_2O_5$ ) was studied in this work the most selective in the catalytic process. Henceforth, the samples prepared by the first method are denoted as **VTm**, where  $m$  is the concentration of  $V_2O_5$  (wt %) in the film of active components, and the samples prepared by the second method are denoted as **VTG**.

The weight of the film of active components was ~3% of the support weight. The samples with  $C_V$  of 3.0, 5.0, 10.0, 20.0, 30.0, 40.0, 50.0, 60.0, 70.0, 80.0, and 90.0% based on the weight of the film of active components were prepared.

The samples were studied by transmission electron microscopy on a JEM-100 CX instrument with an accelerating voltage of 100 kV. Electron microdiffraction was used to determine the structural features and phase composition of particles. The specimens for obtaining microscopic patterns were prepared using alcohol suspensions by ultrasonic dispersion [19]. The surface areas of  $V_2O_5$  were estimated by  $NH_3$  and  $CO_2$  adsorption in a pulse regime [20]. Preliminary experi-

ments showed that in a pulse regime,  $\text{NH}_3$  adsorbs at 100°C only on the surface of  $\text{V}_2\text{O}_5$  and  $\text{CO}_2$  adsorbs at 30°C on the  $\text{TiO}_2$  surface. The surface area of a sample was estimated by comparing the amounts of  $\text{NH}_3$  adsorbed on it and on  $\text{V}_2\text{O}_5$  with the specific surface area determined by nitrogen thermal desorption.

Photoelectron spectra were recorded on an ESCA-3 instrument using  $\text{AlK}\alpha$  radiation without previous treatment of catalysts at a residual pressure in an analyzer chamber of  $5 \times 10^{-9}$  torr [21]. The  $^{51}\text{V}$  NMR spectra were recorded at room temperature on a Bruker MSL-400 spectrometer with a frequency of 105.2 MHz at the pulse width of 1–2  $\mu\text{s}$  and the number of pulses per second of 10 Hz [22]. The ESR spectra were recorded on an ER-200D spectrometer at 77 K with a frequency of 9.3 GHz ( $\lambda = 3.2$  cm). Before the studies by NMR and ESR, the samples were placed in quartz tubes and treated in a helium flow at 350°C for 1 h. Then the samples were moved into quartz ampules without a contact with air, sealed, and introduced into a resonator of the spectrometer.

Before the study of the physicochemical properties, the film of active components was separated from the support.

The catalytic properties of the V/Ti catalysts in durene oxidation were studied on a laboratory flow setup with an integral reactor (catalyst volume was 15  $\text{cm}^3$ ) as well as on a pilot setup with four reaction tubes whose sizes were the same as those of the tubes of the industrial reactor (catalyst volume in one tube was 500  $\text{cm}^3$ ) placed into a salt bath [22]. This allowed the simultaneous study of four samples. The experiments were carried out at atmospheric pressure in the temperature range ( $T_r$ ) of 360–480°C at a durene concentration in a durene–air mixture ( $C_d$ ) of 0.15–0.17 vol % and a space velocity ( $V_d$ ) of 3500–12000  $\text{h}^{-1}$ . The above conditions were close to those of the real industrial process. The rate of non-catalytic durene oxidation was negligibly small. The composition of the oxidation products was determined by GLC using glass capillary columns. The apparent activity of the catalysts was characterized by the minimal temperature of complete durene conversion, and the selectivity of PDMA formation ( $S_p$ ) was evaluated as the PDMA yield based on converted durene.

## RESULTS AND DISCUSSION

As was mentioned above, the structure of the vanadia–titania catalysts depends on their composition and preparation conditions. Our results confirm this statement. Round particles with faceting are present in the sample VT1 (Fig. 1a). According to electron microdiffraction data, the particles are composed of  $\text{TiO}_2$  (anatase). The particle sizes are 30–150 nm. Uniform extinction bands give evidence for the good crystallinity of the particles.  $\text{V}_2\text{O}_5$  particles are not seen in this sample. We suggest that vanadium oxide compounds

are present in a highly dispersed state due to interaction with the surface of  $\text{TiO}_2$ . However, the limited resolution of the electron microscope prevents us from stating the formation of surface vanadium compounds with a thickness of about a monolayer. The low resolution is due to the fact that the atomic weights of vanadium and titanium are close and the ordinal numbers of these elements are small [23].

When  $C_V$  is increased to 3.0 wt %, the needle-shaped particles of the  $\text{V}_2\text{O}_5$  phase appear (Fig. 1b). Their average length is 300 nm, and the thickness is 30–50 nm. In addition to coarse  $\text{V}_2\text{O}_5$  species, round clusters with sizes of up to 3 nm (the largest are 20 nm in size) are seen on the surface of anatase, which also belong to the  $\text{V}_2\text{O}_5$  phase (Fig. 2a). The size and shape of the  $\text{TiO}_2$  (anatase) particles, as well as the needle morphology of the coarse dispersed  $\text{V}_2\text{O}_5$  phase, are almost the same for all samples of the VT $m$  series. The thickness of needles grows with an increase in  $C_V$ . Thus, the thickness of needles in the samples with low  $C_V$  is ~30 nm and increases over 300 nm in the VT60 sample (Figs. 1b–1d). The needles with greater sizes are formed due to the coalescence of fine particles into block structures.

Two types of  $\text{TiO}_2$  particles are found in the sample prepared from a mixture of  $\text{TiO}_2$  (anatase) and  $\text{TiO}_2 \cdot n\text{H}_2\text{O}$  (series VTG) (Fig. 3a). The particles of the first type have a size of ~100 nm and those of the second type are ~20–30 nm joined into agglomerates with a size of 500 nm. Microdiffraction data show that the phase composition of the particles of both types corresponds to anatase. Similarly to the VT $m$  series, the  $\text{V}_2\text{O}_5$  particles of a needle shape with a length up to 100 nm and a width of ~30 nm are found in the samples of the VTG series (Fig. 3b). There are fewer needles and their structure is more perfect than that of the VT $m$  catalysts with the same or higher  $C_V$ . In addition to the particles of the  $\text{V}_2\text{O}_5$  phase, some particles of the  $\text{VO}_2$  phase of a monoclinic modification (m) are seen in the samples of the VTG series.

The high dispersion of  $\text{V}_2\text{O}_5$  in the samples with low  $C_V$  is confirmed by the data on ammonia adsorption. The surface of 1 g of  $\text{V}_2\text{O}_5$  in the sample VT1 is larger than 200  $\text{m}^2$  (Fig. 4). It gradually decreases with increasing  $C_V$  and achieves the value of the surface area of powder  $\text{V}_2\text{O}_5$  in the samples containing more than 30 wt %.

The total surface area of the film of active components passes through a maximum because of a decrease in the dispersion of vanadia compounds with an increase in the  $\text{V}_2\text{O}_5$  content in the catalyst. In the VT $m$  series, the maximum is seen on sample VT20 (Fig. 4).

Note that  $\text{CO}_2$  adsorbs only on the surface of initial  $\text{TiO}_2$  and samples VT1 and VT3. When taking into account that  $\text{CO}_2$  does not adsorb on the surface of  $\text{V}_2\text{O}_5$ , one can conclude that the active component does not cover the support surface in these samples completely even at  $C_V$  that corresponds to several layers (3.0 wt %).

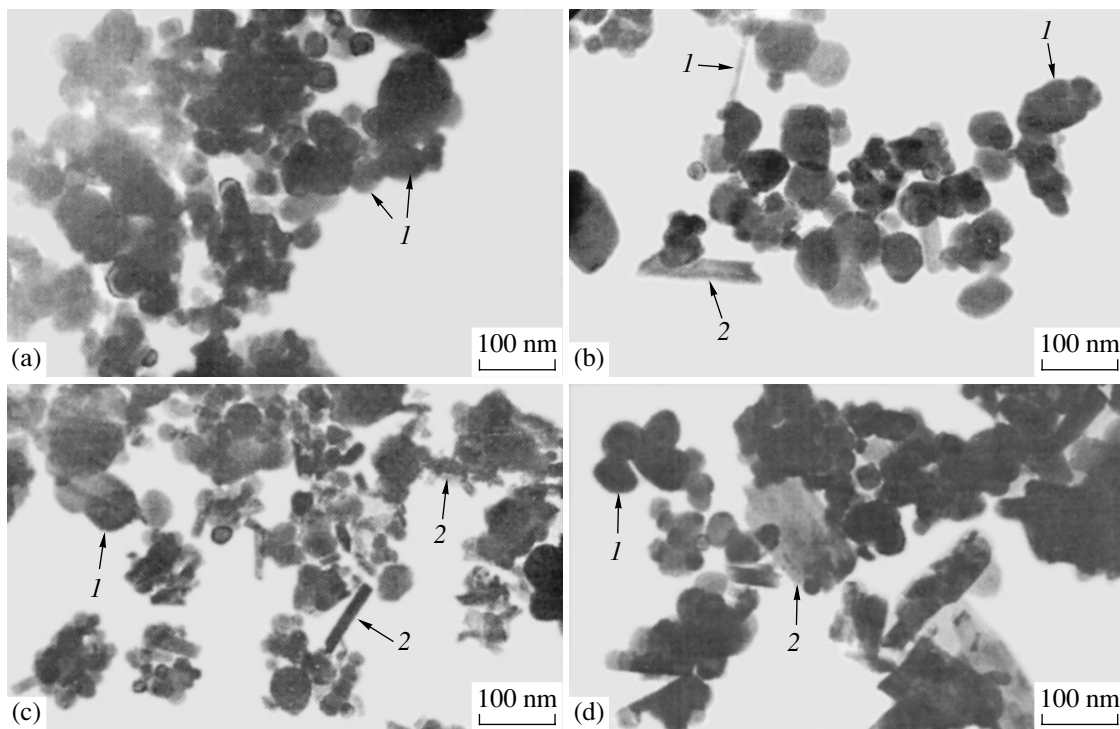


**Fig. 1.** Electron micrographs of initial samples of the VTm series with  $\text{V}_2\text{O}_5$  content, wt %: (a) 1.0, (b) 3.0, (c) 20.0, and (d) 60.0; (1) particles of  $\text{TiO}_2$ , (2) particles  $\text{V}_2\text{O}_5$ .

The state of vanadia compounds in the samples of the VTm and VTG series after their long residence in the reaction medium is substantially different. The VT10 sample after operation for 1150 h contains a great amount of particles of an irregular shape with a size of  $\sim 70$  nm that consist of the  $\text{VO}_2(\text{m})$  with the lattice parameters  $a_0 = 5.743$  Å,  $b_0 = 4.517$  Å,  $c_0 = 5.375$  Å, and  $\beta = 122.6^\circ$  (Fig. 2b) [24]. The structure of  $\text{VO}_2$  is confirmed by electron microdiffraction data. Microdistortions that manifest themselves on the micrographs as curved extinction bands are typical of these particles. The particles of the  $\text{VO}_2(\text{m})$  phase are likely formed by the agglomeration of small crystals upon their reduction in the reaction medium.

The morphology of the particles of the VT20 sample after operation for 1150 h differs from the initial morphology in the appearance of many small particles with a size of at least 50 nm on the surface of anatase in addition to large particles of  $\text{V}_2\text{O}_5$ . The phase composition of these small particles is unknown. Apparently, these particles comprise a reduced form of  $\text{VO}_2(\text{m})$  as in the case of sample VT10 operated for 1150 h.

The VTG sample operated in durene oxidation for 3800 h contains mostly the  $\text{V}_2\text{O}_5$  phase. The amount of the  $\text{VO}_2(\text{m})$  particles is small and slightly differs from that in the initial sample.

The  $^{51}\text{V}$  NMR study [22, 25] of the vanadia-titania systems with low  $C_V$  (less than a monolayer coverage) revealed isolated tetrahedral vanadium complexes,

which were strongly distorted because of the strong binding of vanadium to the  $\text{TiO}_2$  surface through three oxygen atoms. The samples were prepared by the treatment of anatase with  $\text{VOCl}_3$  vapor followed by the removal of physically adsorbed  $\text{VOCl}_3$  and hydroxylation of unreacted V-Cl bonds. The broadened lines in the  $^{51}\text{V}$  NMR spectrum corresponded to these complexes. Such structures were formed at low  $C_V$  and low concentrations of the hydroxyl groups on the anatase surface. At higher  $C_V$ , the above complexes likely began to associate to clusters (sites I). In parallel, clusters of less distorted tetrahedra bound to the  $\text{TiO}_2$  surface through two oxygen atoms (sites II) formed. The signal typical of  $\text{V}_2\text{O}_5$  appeared in the spectra at coverages higher than a monolayer.

The  $^{51}\text{V}$  NMR spectrum of the sample with  $C_V = 1.0$  wt % prepared from well-crystallized anatase with  $S_{\text{sp}} = 8.5 \text{ m}^2/\text{g}$  (sample VT1) (Fig. 5, spectrum 1) differs significantly from the spectra of known pure compounds. The strong broadening of the spectrum does not allow the determination of the number of lines. One can suggest that the spectrum consists of one line with the parameters  $\delta_1 \approx -300$ ,  $\delta_2 \approx -500$ , and  $\delta_3 \approx -1000$  ppm typical of  $\text{V}^{5+}$  tetrahedral complexes that are similar to those found in [22, 25]. The high anisotropy of the spectrum is most probably due to the formation of a vanadium compound whose structure is distorted by strong binding with the  $\text{TiO}_2$  surface.

When  $C_V$  is increased to 3.0 wt % (sample VT3), an additional band appears in the region of  $\delta \approx -315$  ppm

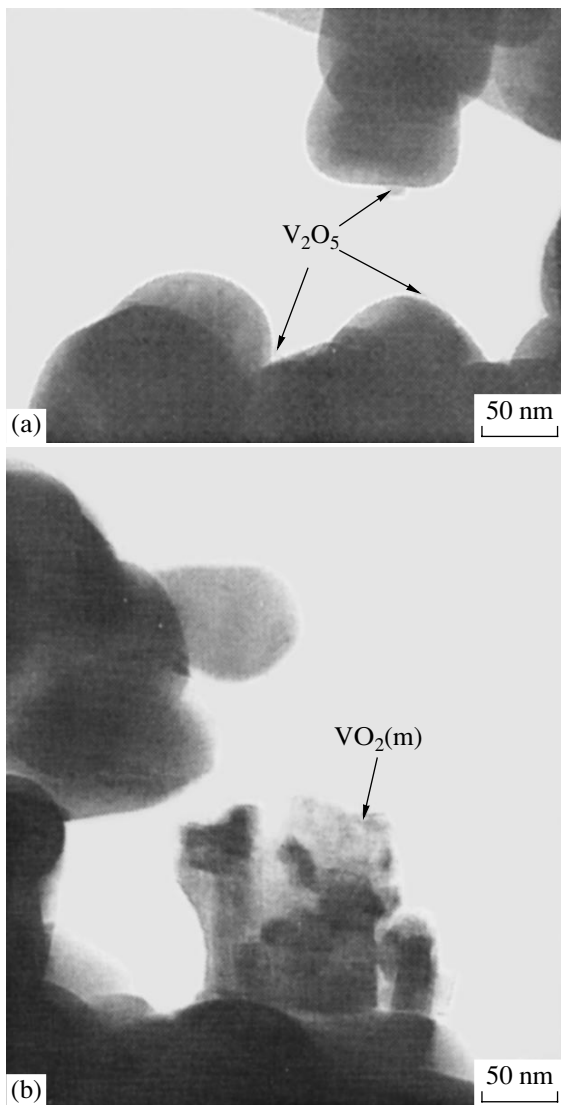


Fig. 2. Electron micrographs of sample VT10 (a) before and (b) after residence in the reaction medium for 1150 h.

(Fig. 5, spectrum 2). The relative contribution of this band increases with increasing  $C_V$ . In the spectrum of the initial sample VT10 (Fig. 5, spectrum 3), the line with axial anisotropy of the chemical shift tensor ( $\delta_1 \approx -315$  ppm,  $\delta_2 \approx -1250$  ppm) is the most pronounced. Comparison with the spectra of known compounds [26] led us to conclude that the compound under consideration is  $\text{V}_2\text{O}_5$ . After prolonged residence of this sample under reaction conditions, the line corresponding to  $\text{V}_2\text{O}_5$  disappears (Fig. 6). The remaining line is close in its parameters to that for a surface compound formed in the  $\text{VT}_m$  samples with low vanadia contents (Fig. 5).

Figure 7 presents the  $^{51}\text{V}$  NMR spectra of the VTG series sample, both initial and spent in the reaction. As can be seen, these spectra are close and correspond to the well-crystallized  $\text{V}_2\text{O}_5$  phase ( $\text{V}_2\text{O}_5$  ( $\delta_1 \approx -315$  ppm,  $\delta_2 \approx -1250$  ppm)). The intensity of the spectrum of the

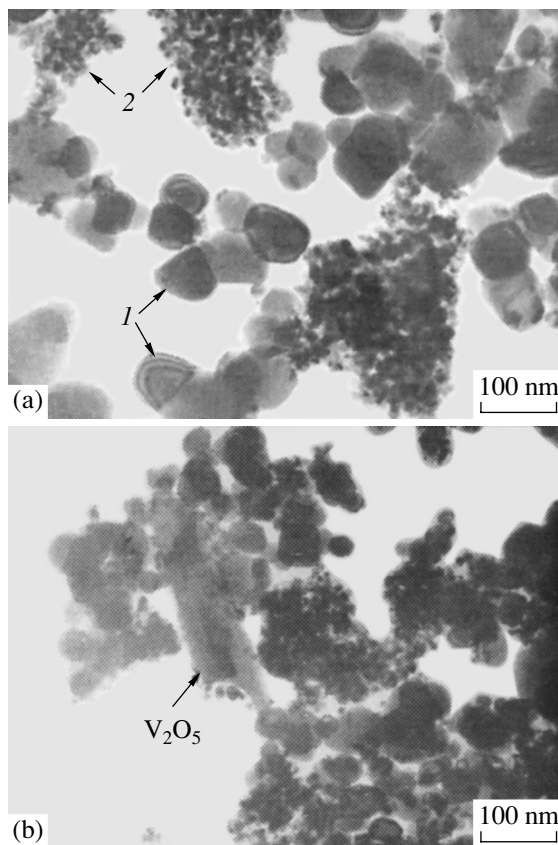
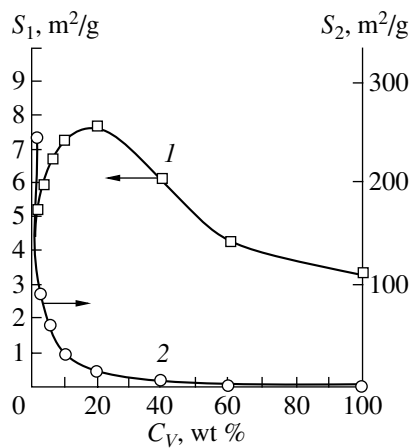


Fig. 3. Electron micrographs of the initial sample of VTG series: (a) particles  $\text{TiO}_2$  (1) coarse particles of  $\text{TiO}_2$  and (2) agglomerates of highly dispersed particles; (b) particles  $\text{V}_2\text{O}_5$ .

spent sample is lower as in the  $\text{VT}_m$  series catalysts, and the line from the surface  $\text{V}-\text{Ti}$  compound is seen in the region of  $-500$  ppm whose relative intensity is higher in the spent sample.

Thus, one can suggest that the surface  $\text{V}-\text{Ti}$  compounds similar to sites I and II described in [22, 25] occur in our samples.

According to the XPS data, the atomic  $\text{V}/\text{Ti}$  ratio in the samples of the VTG series after prolonged residence in the reaction medium changes slightly but decreases 1.5–2.5 times in the  $\text{VT}_m$  series samples. For example, the atomic ratio in VT3 (initial) is 0.30, in VT10 (initial) is 0.58, VT20 (initial) is 1.50, VT20 (50 h of operation) is 0.92, VT20 (1150 h) is 0.59, VT60 is 2.9, VTG (initial) is 0.64, and VTG (3800 h) is 0.59. Since the pore structure of a catalyst after prolonged action of the reaction medium remains unchanged, one can suggest that the distortion and agglomeration of the surface vanadium-containing structures change the  $\text{V}/\text{Ti}$  ratio. This conclusion is confirmed by the electron microscopy. As was mentioned above, the amount of small clusters with a size of  $\sim 3$  nm decreases substantially in the spent VT10 sam-



**Fig. 4.** The specific surface area of  $\text{V}_2\text{O}_5$  as a function of its content: (1) specific surface area based on 1 g of the film of the active components ( $S_1$ ); (2) specific surface area of  $\text{V}_2\text{O}_5$  based on 1 g  $\text{V}_2\text{O}_5$  ( $S_2$ ).

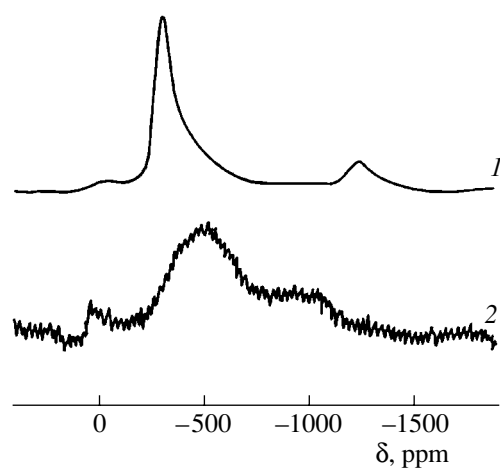


**Fig. 6.** The  $^{51}\text{V}$  NMR spectra of the sample VT10 (1) before and (2) after exposure to the reaction medium for 1150 h.

ple but larger (up to 70 nm) particles of  $\text{V}_2\text{O}_5$  (m) appear.

It follows from NMR (Fig. 7), ESR, and chemical analysis data that a substantial fraction of vanadium in the stable VTG catalyst remains as  $\text{V}^{5+}$  after reaction. Note that  $\text{V}_2\text{O}_5$  in this catalyst is reduced mainly to compounds containing vanadyl ion  $\text{VO}^{2+}$  rather than to  $\text{VO}_2$  (m). The ESR spectrum of  $\text{VO}^{2+}$  is characterized by a hyperfine structure. Only values of  $g_{\perp} = 1.98$  G and  $b_2 = 80$  G were firmly estimated because of the overlapping of different signals.

Thus, the main reason for a change in the structure of the V-Ti catalysts of the  $\text{VT}_m$  series is coarsening of the surface structures of the  $\text{V}^{5+}$  oxide, including the distortion of active surface compounds, which is accompanied by their complete reduction to inactive  $\text{VO}_2$  (m).

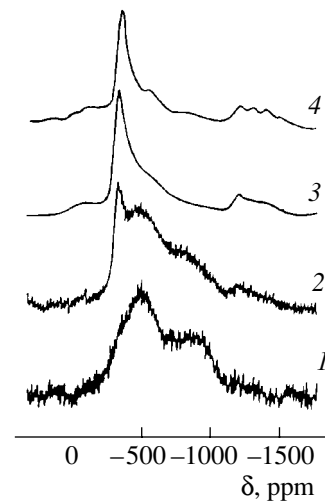


**Fig. 5.** The  $^{51}\text{V}$  NMR spectra of the  $\text{VT}_m$  samples with the  $\text{V}_2\text{O}_5$  content, wt %: (1) 1.0, (2) 3.0, (3) 10.0, and (4) 20.0.

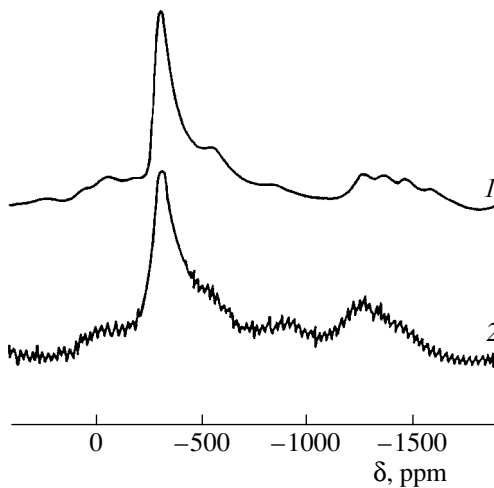


**Fig. 7.**  $^{51}\text{V}$  NMR spectra of the samples of VTG series (1) before and (2) after contact with the reaction medium for 3800 h.

It remains unclear why the catalysts, for example VTG and VT20, with a close chemical composition differ significantly in resistance to agglomeration and reduction. This is probably due to different preparation procedures for these catalysts. When the VTG catalyst is prepared, the support contains hydrated titania along with well crystallized  $\text{TiO}_2$  (anatase). The hydrated titania transforms into anatase upon calcination, and the latter is seen on electron-microscopic patterns as highly dispersed particles. Due to a high content of hydroxyl groups on the surface,  $\text{V}^{5+}$  ions interact with the support to form V-Ti compounds, which cover the surface almost completely. The  $\text{V}^{5+}$  ions in the surface compound coordinate the hydroxyl groups, which interact with the deposited  $\text{V}^{5+}$  compounds to form initially disordered  $\text{V}_2\text{O}_5$  and then, upon calcination, well crystallized  $\text{V}_2\text{O}_5$  particles (Fig. 8, structure a).

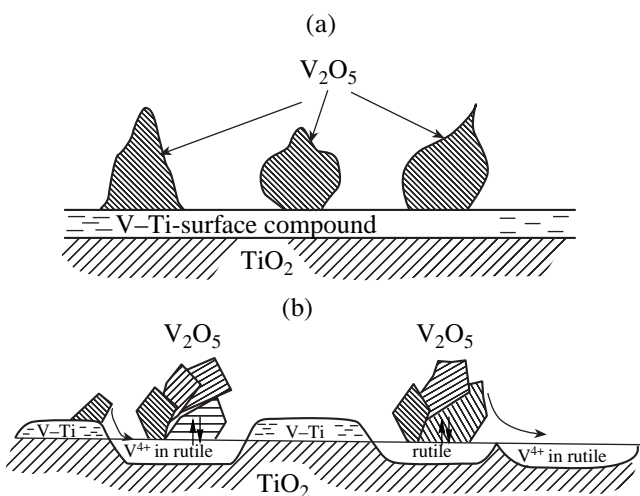


**Fig. 8.** Structures of catalysts (a) VTG and (b) VTm. Diffusion of particles to form a solid solution of  $V^{4+}$  in rutile is shown by arrows.

Such efficient interaction is absent in the case of the VTm catalysts. Despite the excess of  $V_2O_5$ , the active surface phase exists in the form of distinct islands on the support. According to the X-ray diffraction data, a small amount of rutile is present in the VTm samples. Rutile as a thermodynamically more stable phase is located mostly on the surface, and a solid solution of  $V^{4+}$  ions in rutile is formed upon the deposition of  $V_2O_5$ . Therefore, a fraction of  $V^{5+}$  in the form of surface monolayer compounds in the VTm samples is substantially smaller than in the VTG sample. Most of  $V^{5+}$  is distributed over the free surface as blocks of large needle crystals of  $V_2O_5$  that are formed by the coalescence of smaller needles. In addition, the interaction between  $V^{5+}$  and the support on the interface during calcination of the sample can produce a small amount of the  $V^{4+}$  solid solution in rutile. The signals typical of the  $V^{4+}$  solid solutions in rutile were found in the ESR spectra of the initial VTm samples. These were lines with a hyperfine structure and the following parameters of hyperfine interaction:  $A = 160$  G and  $B = 30$  G. The  $q_{\perp}$  and  $q_{\parallel}$  values were not estimated because of signal overlap. The  $V^{4+}$  concentration was several percents of  $C_V$ . Taking into account the low specific surface areas of the VTm samples and the fact that the main amount of vanadium occurs as  $V_2O_5$  large crystallites, the fraction of the surface occupied by the solid solution can reach significant values (Fig. 8, structure b).

More regular  $V_2O_5$  particles are formed by interaction between  $V^{5+}$  and hydroxyl groups, which are nearly absent from the surface of the VTm samples, and hence the contribution of chemical interactions is small. Therefore,  $V_2O_5$  is randomly distributed over the surface. Unlike VTG, the  $V_2O_5$  crystals in the VT20 and VT60 samples have a pronounced block structure formed by the coalescence of closely located small  $V_2O_5$  crystallites.

The agglomeration of  $VO_2$  particles after prolonged exposure to the reaction mixture can be described as follows. The  $V^{4+}$  ions of a solid solution in rutile diffuse to the surface and serve as the centers of V(IV) crystallization to the  $VO_2$  monoclinic structure. When  $V^{4+}$  ions move from positions typical of the rutile structure, the  $VO_2$  (m) phase can nucleate on the  $TiO_2$  surface. It is known that the transition from the tetragonal structure ( $V^{4+}$  in rutile) to the monoclinic one occurs readily and does not require significant lattice reconstruction [27]. This suggestion agrees with ESR data for the spent VT20 sample, which reveal a decrease in the  $V^{4+}$  concentration both in the solid solution and in the form of the isolated  $VO_2^{2+}$  particles. The diffusion of  $V^{4+}$  to this center is likely a rate-determining stage. Diffusion can occur more rapidly when  $V_2O_5$  crystals are located directly on the surface region occupied by the solid solution. In addition, growing  $VO_2$  crystals can "withdraw" the  $V^{4+}$  ions, formed during reaction, from the surface sites. This process is slower than the above process because it requires the rupture of chemical bonds.

The structure in which vanadium of the V-Ti surface compounds is bound to the support (anatase) and  $V_2O_5$  via chemical bonds and the above centers of crystallization are absent is more stable. In this structure,  $V_2O_5$  can partially be reduced to the equilibrium amount of  $VO_2^{2+}$  (under reaction conditions). Structure (a) is usually present in the VTG sample on the  $TiO_2$  small particles that are formed from titania hydrate, and structure (b) is present in the VTm and VTG samples on the coarsely dispersed  $TiO_2$  particles.

#### Catalytic Properties of the Vanadia-Titania Catalysts

A change in the state of a catalyst and, as a consequence, its catalytic behavior in the reaction medium is a common phenomenon in heterogeneous catalysis [18, 28, 29]. It follows from our findings that this is also characteristic of vanadium-containing catalysts in durene oxidation. For example, the activity of a sample containing only  $V_2O_5$  ( $V_2O_5$ /porcelain) increases during the first hours of the experimental run. This is evidenced by a monotonous increase in the durene conversion ( $X_d$ ), which achieves 100% in 8 h at 410°C and  $V_d = 5000$  h<sup>-1</sup> (Table 1). Then the activity does not change over the test period (1500 h).

A growth of durene conversion is accompanied by an increase in the selectivity to PMDA ( $S_p$ ) due to the transformation of the products of the partial oxidation of the raw material to PDMA. The maximal value of  $S_p$  equal to 42–43 mol % is achieved in 12 h (Fig. 9, curve 1) and remains constant for the next 5–10 h. Then, the conversion decreases because of the formation of the products of complete oxidation and achieves ~36–38 mol % in 40–44 h of operation. When the oxidation period increases further,  $S_p$  does not change.

When this sample is additionally treated thermally at 600°C for 2 h, its initial activity decreases compared

to that of the  $\text{V}_2\text{O}_5$ /porcelain sample calcined at 450°C for 9 h. As a result, the time for achieving 100% conversion and a stationary state of the catalyst increases under the same conditions of oxidation. Note that the maximal  $S_p$  is higher and equals 51–56 mol %. However, it decreases to ~38 mol % when the stationary state is achieved (Fig. 9, curve 2).

When the  $\text{V}^{5+}$  ions in the  $\text{V}_2\text{O}_5$ /porcelain sample calcined at 450°C for 9 h are reduced to  $\text{V}^{3+}$  in a hydrogen flow, the catalyst becomes more active but poorly selective to PDMA. Complete durene conversion over this sample is found already 2 h after the onset of the process but  $S_p$  is only 10–12 mol % (Fig. 9, curve 3). Other reaction products consist of carbon oxides and water. With time,  $S_p$  increases to the stationary values found for other samples.

Thus, a change in the temperature of preliminary calcination and treatment in the oxidative medium result in the  $\text{V}_2\text{O}_5$ /porcelain samples, which essentially differ in their initial catalytic behavior. However, this difference disappears in several tens of hours of durene oxidation under conditions close to industrial ones. The stationary state of the catalyst is achieved in which  $S_p$  is lower than the maximal  $S_p$  found under the conditions used in this work.

The above findings indicate that the lower  $S_p$  value for the  $\text{V}_2\text{O}_5$ /porcelain catalyst in the stationary state is due to its deep reduction. The question arises as to why the reduction of  $\text{V}^{5+}$  to  $\text{V}^{4+}$  and  $\text{V}^{3+}$  decreases  $S_p$ . We have found [30] that the reduction of  $\text{V}_2\text{O}_5$  leads to an increase in the concentration of adsorption sites for a hydrocarbon capable of forming strongly adsorbed hydrocarbon complexes, which are not desorbed from the catalyst surface in the absence of oxygen in the gas phase even at 400°C. When oxygen is fed, these complexes interact with oxygen and transform into carbon oxides and water probably through carbonate-carboxylate structures or carbonyl and peroxide compounds [29]. This suggests the participation of both gas-phase oxygen and weakly bound oxygen of the catalyst lattice.

The catalytic behavior of the V-Ti systems with  $C_V$  greater than 30 wt % do not differ from that of the  $\text{V}_2\text{O}_5$ /porcelain catalyst.  $\text{TiO}_2$  does not catalyze durene oxidation under the conditions studied. The V-Ti systems with  $C_V$  from 1 to 30 wt % are more active than

the  $\text{V}_2\text{O}_5$ /porcelain samples, and durene is completely converted under milder conditions. The minimal  $T_r$  for the VT20 sample at which  $X_d = 100\%$  is lower by 50°C than that for the  $\text{V}_2\text{O}_5$ /porcelain sample at the same contact times. The higher activity of the V-Ti systems is due to the formation of the surface vanadia-titania compounds [25].

The activation of these systems differs from that for the  $\text{V}_2\text{O}_5$ /porcelain described above. Under the experimental conditions,  $X_d = 100\%$  is achieved in the first hours of the experiment and  $S_p$  increases during 5–10 h (Fig. 10) with a simultaneous decrease in the yield of the products of complete durene oxidation. On the sample containing only  $\text{V}_2\text{O}_5$ ,  $S_p$  passes through a maximum when the catalyst reaches the stationary state (Fig. 9), which is due to  $\text{V}_2\text{O}_5$  deep reduction. This is accompanied by the appearance of the sites for complete durene oxidation. The absence of a similar maximum in the case of the V-Ti systems with  $C_V$  from 1 to 30 wt % is explained by the fact that the degree of reduction of these systems by the reaction medium is lower because of the higher rates of reoxidation of  $\text{V}^{3+}$  ions, which at least partially enter the highly dispersed surface structures. In addition, the high surface area of the active component in the V-Ti systems (Fig. 4) determines a lower “durene load” per surface unit and consequently a lower degree of  $\text{V}^{5+}$  reduction. An increase in  $S_p$  during the initial hours of durene oxidation is due to the removal of weakly bound oxygen, responsible for complete oxidation, from the catalyst.

The selectivity of the V-Ti systems that achieved the stationary state is primarily determined by the catalyst composition. The selectivity increases to 58–60 mol % with increasing  $C_V$  from 1 to 20 wt % (Fig. 11). With a further increase in  $C_V$  to 30 wt %,  $S_p$  does not change and then gradually decreases to the value characteristic of the  $\text{V}_2\text{O}_5$ /porcelain sample.

Both the higher activity of a series of vanadia-titania catalysts and their higher  $S_p$  compared with  $\text{V}_2\text{O}_5$  are likely due to the fact that the surface vanadia-titania compounds (sites I and II) are formed upon the deposition of  $\text{V}_2\text{O}_5$  onto the  $\text{TiO}_2$  (anatase) surface and the concentration of these sites depends on  $C_V$ . As was mentioned above, sites I are formed at low  $C_V$  (samples VT1 and VT3). At higher  $C_V$  (samples VT3, VT5, etc.), sites II appear. According to [22, 25], sites I are respon-

**Table 1.** Durene conversion on the  $\text{V}_2\text{O}_5$ /porcelain catalyst with time ( $T_r = 410^\circ\text{C}$ ,  $C_d = 0.14$  vol %,  $V_d = 5000 \text{ h}^{-1}$ )

Characteristics of sample	Conversion, mol %			
	time, h			
	2	4	8	12
Calcined in air at 450°C for 4 h	71.1	92.2	100	100
Calcined additionally at 600°C for 2 h	60.8	72.6	91.5	100
Reduced in a $\text{H}_2$ flow at 450°C for 2 h	100	100	100	100

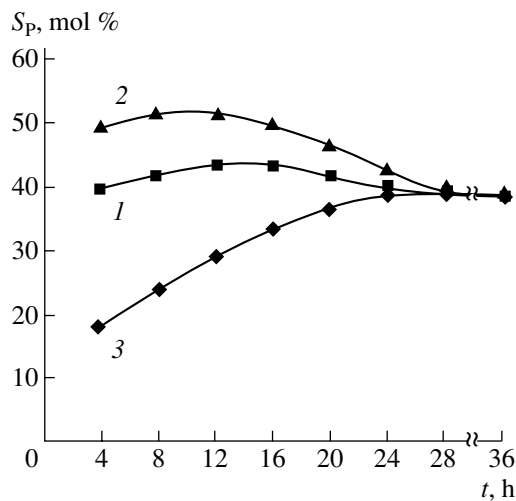


**Fig. 9.** A plot of  $S_p$  in durene oxidation over the  $V_2O_5$ /porcelain catalyst vs. time ( $T_r = 410^\circ C$ ,  $C_d = 0.14$  vol %,  $V = 5000$   $h^{-1}$ ): (1) sample was calcined in air at  $450^\circ C$  for 9 h; (2) sample is additionally calcined at  $600^\circ C$  for 2 h; and (3) sample is reduced in a  $H_2$  flow at  $450^\circ C$ .

sible for complete *o*-xylene oxidation and sites II are responsible for its oxidation to phthalic anhydride. Taking into account the structural similarity of durene and *o*-xylene molecules, one can suggest that durene is also oxidized to carbon oxides and water on sites I and to PMDA on sites II. Durene molecules are adsorbed on sites II through the activation of the  $CH_3$  groups with the participation of the OH groups bound with  $V^{5+}$ , and this is accompanied by the reduction of  $V^{5+}$  to  $V^{3+}$ . The active sites are rapidly reoxidized with oxygen of the gas phase, and the products of partial durene oxidation and water are simultaneously desorbed. The participation of  $V_2O_5$  mobile oxygen in the reoxidation of the surface site is also possible. The  $V_2O_5$  phase is formed simultaneously with sites I and II and barely affects the activity and selectivity of the V-Ti catalytic systems. The ratio between sites I and sites II changes with  $C_V$  in favor of sites II, and this is likely the reason for the  $S_p$  increase. With a further increase in  $C_V$ ,  $S_p$  does not change in some range of  $C_V$  and then decreases because of blocking the V-Ti compounds by large  $V_2O_5$  crystallites. As a result, a maximum appears on the curve describing  $S_p$  as a function of  $C_V$ . Note that after reaching the stationary state of the VT20 and VTG samples, their activities become close, and the maximal selectivities  $S_p$  become 58–60 and 65–57%, respectively.

At a constant composition of the catalyst,  $S_p$  depends on the conditions of durene oxidation. This is 54.6 mol % for the VT20 sample at  $390^\circ C$  and a space velocity of  $7000$   $h^{-1}$ . With increasing temperature to  $410^\circ C$ ,  $S_p$  increases to 59.0 mol %. A further increase in temperature results in a decrease in  $S_p$ . This character of  $S_p$  variation with temperature is found for all samples and is explained by the fact that the rates of the stages of the conversion of intermediates to PMDA increase

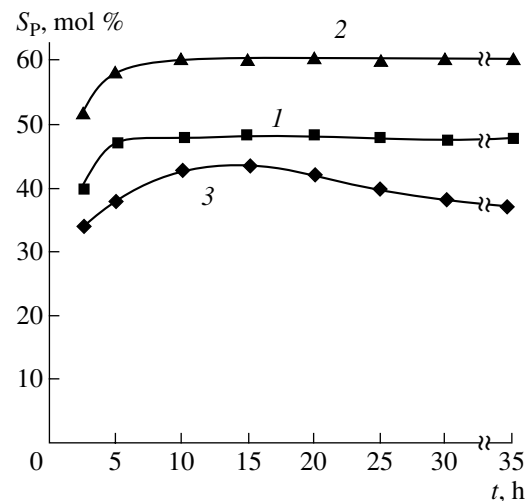


**Fig. 10.** Plot of  $S_p$  in durene oxidation over the V-Ti catalysts of VT $m$  series vs. time ( $T_r = 410^\circ C$ ,  $C_d = 0.14$  vol %,  $V = 5000$   $h^{-1}$ ,  $X_d = 100\%$ ): (1) VT5, (2) VT20, and (3) VT40, VT60.

with increasing temperature. PMDA is resistant to oxidation to  $CO_2$  at temperatures up to  $430^\circ C$ . At higher temperatures, the oxidation rate of PMDA to  $CO_2$  increases and  $S_p$  decreases.

Note that the thermal treatment of the VT $m$  and VTG samples in air at  $600^\circ C$  for 2 h results in their irreversible deactivation because of sintering of the surface structures and the partial interaction of vanadium cations with  $TiO_2$  to form solid solutions [12].

Whereas the activities and  $S_p$  for the VT20 and VTG samples in durene oxidation are close after the stationary state is reached, their stabilities differ significantly. The catalytic behavior of the VTG samples in durene oxidation does not change even in  $3800$  h (Table 2).

The stability of the VT $m$  samples is markedly lower. After  $400$  h of operation,  $S_p$  on the VT10 catalyst is 43–45 mol % at the complete durene conversion (Table 2). This  $S_p$  is close to the maximal value found for VT10. However, after  $1150$  h, it decreases to 28–30 mol % because of the enhancement of the complete durene oxidation; that is, the catalyst deactivates. Note that an attempt to reactivate the catalyst by treatment in air at  $450$ – $500^\circ C$  failed.

An increase in the  $V_2O_5$  concentration to 20 wt % at the same preparation procedure (VT20) did not improve the catalyst stability, although the PMDA yield in durene oxidation was 58–60 mol % in  $400$  h. As was mentioned, a further increase in the  $V_2O_5$  content to 60 wt % results in the catalyst close to  $V_2O_5$  in properties. The catalyst is stable but less active and selective than the optimal vanadia–titania samples.

Thus, when vanadia–titania catalysts are prepared using well crystallized  $TiO_2$  (anatase) with low concentration of the surface OH groups and rutile additives,

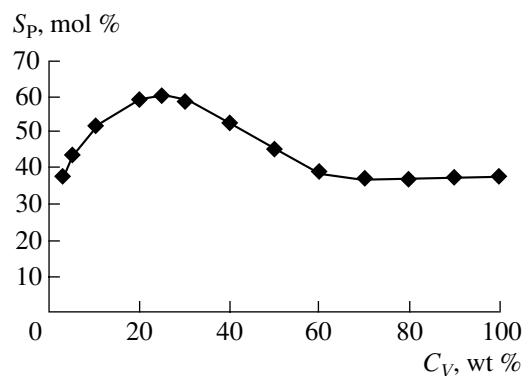


**Fig. 11.** Plot of  $S_p$  in durene oxidation over the V-Ti catalysts of BTm series vs.  $V_2O_5$  content.  $T_r = 410^\circ\text{C}$ ,  $C_d = 0.14$  vol %,  $V = 5000 \text{ h}^{-1}$ ,  $X_d = 100\%$ .

the formation of active vanadia-titania compounds is hampered and their concentration is small. Vanadium is present mostly in the form of  $V_2O_5$  crystallites and  $V_2O_5$  solid solutions in rutile. These catalysts are unstable during prolonged durene oxidation.

When a mixture of  $TiO_2$  (anatase) and hydrated highly dispersed  $TiO_2 \cdot nH_2O$  is used as a support, the vanadium and OH groups interact on the surface to form surface V-Ti compounds, which determine the catalytic behavior of the sample. Under these conditions, the catalyst is stable over a long period of performance.

TO conclude, let us discuss the role of excess (relatively to a monolayer of V-Ti compound)  $V_2O_5$  in the vanadia-titania catalysts. Comparison of their catalytic properties with those of  $V_2O_5$ /porcelain in durene oxidation allows us to conclude that the presence of crys-

**Table 2.** Catalytic properties of various samples vs. time of durene oxidation ( $C_d = 0.14$  vol %,  $V_d = 9000 \text{ h}^{-1}$ )

Sample	Temperature of complete conversion, $^\circ\text{C}$	$S_p$ , mol %
After 400 h oxidation		
VT10	390	43–45
VT20	390	65–67
VT60	430	40–41
VTG	390	65–67
After 1150 h oxidation		
VT10	430	28–30
VT20	430	28–30
VT60	430	40–41
VTG	390	65–67
After 3800 h oxidation		
VT60	430	40–41
VTG	390	65–67

talline  $V_2O_5$  in these catalysts does not affect substantially their activity and  $S_p$ . Nevertheless, it is well known that practically all industrial catalysts contain a substantial amount of excess  $V_2O_5$  (from 5.0 to 25.0 wt %), although ~3 wt %  $V_2O_5$  is sufficient for the monolayer coverage of the surface with  $S_{sp} \approx 30 \text{ m}^2/\text{g}$ . This can be associated with the fact that excess vanadia is needed to form a monolayer in industrial catalysts because of the nonuniformity of coverage caused by the preparation procedure. However, we cannot rule out that the presence of  $V_2O_5$  in the surface structures can improve the stability of their operation due to mobile oxygen, which is retained at the high degree of oxidation of vanadium cations in the surface V-Ti compounds.

#### ACKNOWLEDGMENTS

We are grateful to V.I. Zaikovskii, A.V. Kalinkin, O.B. Lapina, and L.G. Pinaeva, (Boreskov Institute of Catalysis, Siberian Division, Russian Academy of Sciences) and F.G. Arslanov (Pilot plant NIINeftekhim, Ufa) for their assistance in experiments and useful discussions.

#### REFERENCES

1. Borshchenko, V.P. and Makhiyanov, G.F., *Piromellitovyi diangidrid* (Pyromellitic Dianhydride), Moscow: TsNIITENeftekhim, 1974.
2. Dias, C.R., Portela, M.F., and Bond, G.C., *Catal. Rev. – Sci. Eng.*, 1997, vol. 39, no. 3, p. 169.
3. Suvorov, B.V., Sembaev, D.Kh., and Kogarchinskii, A.D., *Izv. Akad. Nauk KazSSR, Ser. Khim.*, 1974, vol. 39, no. 10, p. 14.
4. US Patent 4582912.
5. Churkin, Yu.V., Balaev, A.V., Svirskaya, M.M., and Egorov, I.V., *Khim. Prom-st.*, 1989, no. 7, p. 487.
6. Bond, G.C., Zurita, J.P., Flamerz, S., et al., *Appl. Catal.*, 1986, vol. 22, p. 361.
7. Busca, G., Marchetti, L., Centi, G., and Trifiro, F., *J. Chem. Soc., Faraday Trans. I*, 1985, vol. 81, p. 1003.
8. Cartan, F. and Caughlan, C.N., *J. Phys. Chem.*, 1983, vol. 64, no. 12, p. 5176.
9. Hengstum, A.J., Van Ommen, J.G., Van Bosch, H., and Gellings, P.J., *Appl. Catal.*, 1983, vol. 5, no. 1, p. 207.
10. Pinaeva, L.G., Sai Prasad, P.S., Balzhinimaev, B.S., et al., *React. Kinet. Catal. Lett.*, 1988, vol. 36, no. 1, p. 229.
11. Wachs, I.E., Saleh, R.Y., Chan, S.S., and Chersich, C.C., *Appl. Catal.*, 1985, vol. 15, no. 1, p. 102.
12. Saleh, R.Y., Wachs, I.E., Chan, S.S., and Chersich, C.C., *J. Catal.*, 1986, vol. 98, no. 1, p. 102.
13. Miyata, H., Nakagawa, Y., Ono, T., and Kubokawa, Y., *Chem. Lett.*, 1983, p. 1141.
14. Cristiani, C., Forzatti, P., and Busca, G., *J. Catal.*, 1989, vol. 116, no. 2, p. 586.
15. Nag, N.R. and Massoth, F.E., *J. Catal.*, 1990, vol. 124, no. 1, p. 127.
16. Went, G.T., Oyama, S.T., and Bell, A.T., *J. Phys. Chem.*, 1990, vol. 94, no. 10, p. 4240.

17. Davydov, A.A., *Kinet. Katal.*, 1993, vol. 34, no. 6, p. 1056.
18. Alkhazov, T.G. and Margolis, L.Ya., *Vysokoselektivnye katalizatory okisleniya uglevodorodov* (Highly Selective Catalysts for Hydrocarbon Oxidations), Moscow: Khimiya, 1988.
19. Zenkovets, G.A., Gavrilov, V.Yu., Kryukova, G.N., and Tsybulya, S.V., *Kinet. Katal.*, 1997, vol. 39, no. 1, p. 122.
20. Belokopytov, Yu.V., Khalyavenko, K.M., and Rubanik, M.L., *Kinet. Katal.*, 1973, vol. 14, no. 5, p. 1280.
21. Pinaeva, L.G., Rar, A.A., Kalinrin, A.V., *et al.*, *React. Kinet. Catal. Lett.*, 1990, vol. 41, no. 2, p. 375.
22. Pinaeva, L.G., Lapina, O.B., Mastirhin, V.M., *et al.*, *J. Mol. Catal.*, 1994, vol. 88, p. 311.
23. Speis, Dzh., *Eksperimental'naya elektronnaya mikroskopiya* (Experimental Electron Microscopy), Moscow: Mir, 1985.
24. ASTM, *Powder Diffraction File, Inorganic*, ICPDS, 1977.
25. Pinaeva, L.G., *Cand. Sci. (Chem.) Dissertation*, Novosibirsk: Inst. Catal., 1997.
26. Bugaev, A.A., *Fazovyi perekhod metall-poluprovodnik i ego primenenie* (Metal–Semiconductor Phase Transition and its Application), Leningrad: Nauka, 1979.
27. Eckert, H. and Wachs, I.E., *J. Phys. Chem.*, 1989, vol. 93, p. 6797.
28. Krylov, O.V., *Kinet. Katal.*, 1981, vol. 22, no. 1, p. 15.
29. Boreskov, G.K., *Geterogennyi kataliz* (Heterogeneous Catalysis), Moscow: Nauka, 1986.
30. Frolova, L.V., *Cand. Sci. (Eng.) Dissertation*, Ufa: Inst. Petrochem. Catal., 1987.